Sensitivity of NLTH Analysis of MDOF Bridges to Choice of Viscous Damping Models.

Arjun Jayaprakash

April 27, 2017

Abstract

42 NLTH analysis were performed on MDOF bridge fiber based models, each analysis having a different combination of specified variables. The variables were classified based on bridge geometry (2 models), ground motion intensity (3 intensities), abutment fixity conditions (2 conditions) and viscous damping models (4 models). The results were used to assess the sensitivity of response prediction to use of different viscous damping models. It was found that the responses are sensitive to the choice of damping models. The study could also reveal some patterns that can be used to make decisions as to what approach need be used and where to be cautious about in more comprehensive studies in the future.

1 Introduction

There has been a rising interest among engineers to conduct non-linear time history (NLTH) analysis as part of the seismic design procedure for bridges. A good understanding of member parameters such as strength, stiffness and damping are crucial for accurate results from NLTH analysis. Strength and stiffness in dynamic analyses are well understood but the viscous damping model that is mostly being used in commercial analysis programs, namely initial stiffness proportional Rayleigh damping, is questionable. This model prescribes a constant damping matrix proportional to the initial stiffness matrix of a structure. Theoretically, this is inaccurate because of three main reasons.

1. Elastic viscous damping that accounts for material damping in the elastic range is not required to continue the same function in the inelastic range where hysteretic damping exists.
2. Since the stiffness of the system changes in the inelastic range, an argument can be made against the use of a constant damping proportional to initial stiffness.
3. Elastic viscous damping also accounts for energy dissipation by the foundation (mainly in bridges). Since the demand going into the foundation remains constant after yielding, using the same damping in the inelastic range is erroneous.

Albeit, the above can be stated in theory, if the sensitivity of response prediction to the variation in damping models is minor, the simplest model would serve the purpose. Sensitivity of displacement predictions of SDOF systems to choice of initial stiffness and tangent stiffness proportional damping models in NLTH analysis have been studied in the past([3],[6] and [7]). It was found that the results vary considerably, with the tangent stiffness proportional model better representing actual tests. This project makes an effort towards understanding the sensitivity of response predictions of MDOF systems to the choice of four different damping models in NLTH analysis.

2 Viscous damping in NLTH Analysis

2.1 Analysis of SDOF systems

Single degree-of-freedom (SDOF) non-linear equation of motion is of the form:

$$m\ddot{u} + c\dot{u} + f(k,u) = -m\ddot{u_g} \tag{1}$$

where m,c and k represent the mass, damping constant and stiffness of the structure. $\ddot{u}, \dot{u}$ and u are the acceleration, velocity and displacement respectively. $\ddot{u_g}$ is the ground acceleration. Non-linear time history (NLTH) analysis is carried out by direct integration of the equation of motion using time-stepping schemes and

non-linear iteration techniques. The elastic damping, c, is commonly modeled using initial stiffness damping. A single value of the damping constant c is used throughout the analysis.

$$c = 2m\omega_i\xi \tag{2}$$

where, ω_i is the fundamental circular frequency of the SDOF structure, m is the mass and ξ is the specified damping ratio.

An alternative way to model elastic damping is by using tangent stiffness proportional damping. Here, the damping constant, c_t is proportional to the instantaneous stiffness value k_t.

$$c_t = 2\xi\sqrt{mk_t} \tag{3}$$

In this case, the value of c_t changes in every time step. From [3],[6] and [7] it is evident that tangent stiffness proportional damping is the more appropriate damping model for SDOF systems. A sample result showing the time-history responses obtained using initial stiffness and tangent stiffness proportional damping is shown in Figure 1a. The shake table experiment by [6] has shown that tangent stiffness proportional damping does a much better job of predicting close to actual response compared to initial stiffness proportional damping. This is clearly illustrated in Figure 1b. As of now, it is considered that the same may be appropriate for MDOF systems as well.

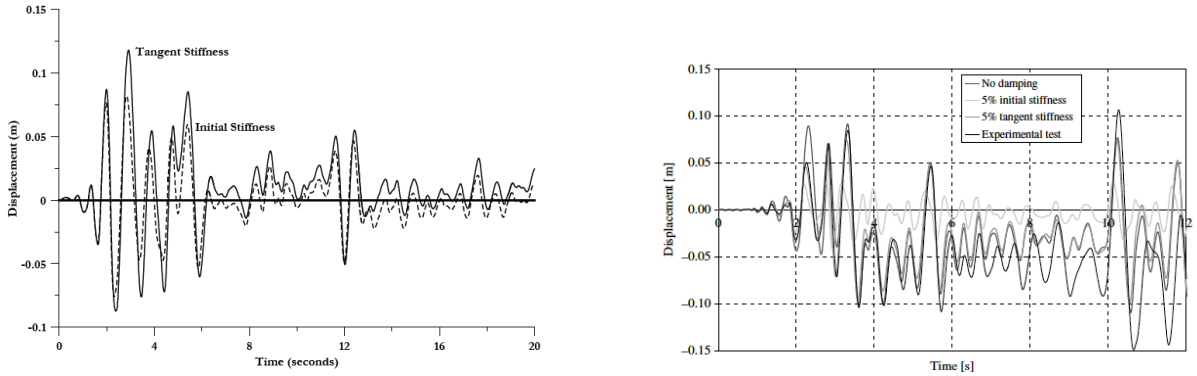

(a) (b)

Figure 1: (a) Figure shows a sample time-history response of an SDOF system using both initial stiffness proportional and tangent stiffness proportional damping (from Priestley and Grant[7], 2005). (b) Figure shows the results of an actual SDOF shake table experiment compared with numerical predictions (from Petrini et al.[6], 2008).

2.2 Analysis of MDOF systems

After the shake table experiment by [6], it was assumed that a similar damping model may suffice in predicting non-linear response of MDOF structures. Albeit a logical conclusion, engineers may be faced with a different problem for MDOF systems. Unlike SDOF systems, MDOF systems do not have a single value of damping constant. Non-linear analysis requires us to specify a damping matrix to carry out direct integration of the MDOF equation of motion. Among various methods to assemble a reasonable damping matrix, the most common one in use in almost all analysis software is the Rayleigh damping model.

Rayleigh damping matrix $\boldsymbol{C}$ is obtained by a combination of a mass proportional and a stiffness proportional component

$$\boldsymbol{C} = a_0\boldsymbol{M} + a_1\boldsymbol{K} \tag{4}$$

where $\boldsymbol{M}$ is the mass matrix and $\boldsymbol{K}$ is the stiffness matrix. The damping ratio for the nth mode of the system is:

$$\xi_n = \frac{a_0}{2\omega_n} + \frac{a_1}{2}\omega_n \tag{5}$$

where ω_n is the circular frequency of the nth mode. Typically, two frequencies are chosen by the engineer to create two equations to solve for a_0 and a_1. These constants are then used to create the $\boldsymbol{C}$ matrix. As per the discussion earlier, an appropriate way to use this would be to combine the mass proportional component to the stiffness proportional component at every time step as the stiffness matrix varies in the non-linear analysis. One

of the concerns regarding the use of this method is the effective distribution of the specified damping between the mass and stiffness components. [7] provides the following example. If the two chosen frequencies are those that correspond to, say, $T_1 = 1.5$ sec and $T_2 = 0.3$ sec, even if a 5% tangent stiffness proportional damping is specified, only 0.83% is stiffness proportional and 4.17% is mass proportional. This means that the system will behave similar to initial stiffness proportional damping even in the non-linear range. Further study is required to ascertain the effects of this. Problems with use of Rayleigh damping have also been pointed out in [1] and [2].

3 Non-linear time history analysis of MDOF bridges

3.1 Bridge models

Two 3-span bridges were modeled using a fiber based modeling program (SEISMOSTRUCT[8]) for this study (Figure 2).

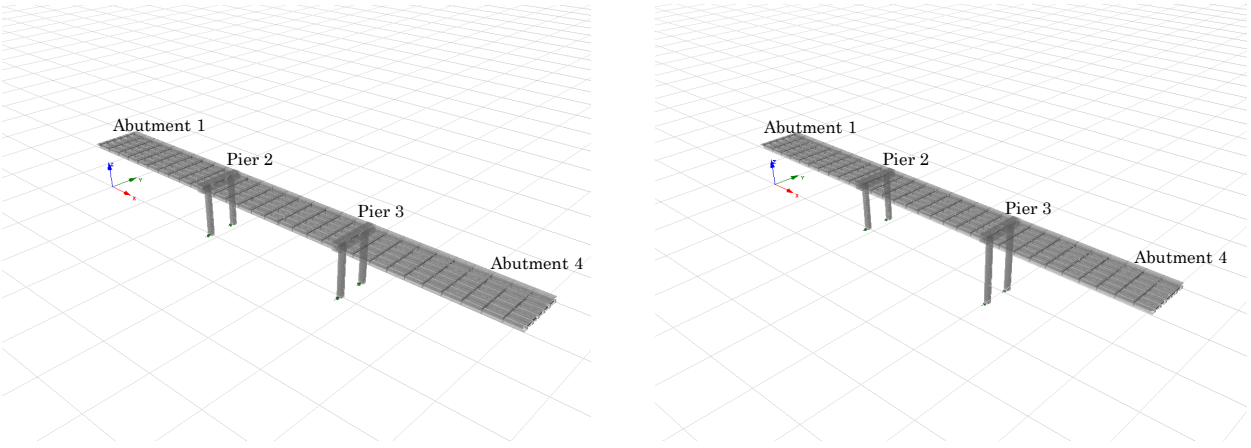

(a) (b)

Figure 2: Figure shows the two different bridge models used for this study (a) Bridge 1 and (b) Bridge 2.

The bridges were of three equal spans of 36.5 m and the only difference between the two models was the height of Pier 3. Bridge 1 had both piers of the same height of 13 m. As a consequence Bridge 1 was symmetric. For Bridge 2, the height of Pier 2 was 13 m and of Pier 3 was 18 m making the bridge asymmetric. A comparison of responses between the two was done to understand the behavior of a regular bridge to a slightly irregular one. The natural time periods of the bridges also vary. Bridge 2 had a higher time period. It has to be noted here that the fundamental time period for each model was obtained by an eigenvalue analysis of the structure using reduced stiffness properties (0.5 EI for columns and 1.0 EI for cap beam and girders). See Table 1 for details.

Characteristic	Bridge 1	Bridge 2
Span length (m)	36.5	36.5
Pier 2 height (m)	13	13
Pier 3 height (m)	13	18
Fundamental Period (Free abutment) (s)	1.60	2.08
Fundamental Period (Restrained abutment) (s)	0.70	0.84

Table 1: Characteristics of the two bridge models used in this study.

The columns were defined using the displacement-based non-linear frame element. Concrete material properties used were f'_c=28 MPa, Modulus of Elasticity, E=24870.06 MPa and Mander model [4] for concrete non-linear concrete stress-strain relationship. The reinforcement steel properties used were f_y=420 MPa, Modulus of Elasticity, E=200015.914 MPa and the Menegotto-Pinto model [5] for non-linear stress-strain relationship with strain hardening parameter = 0.005.

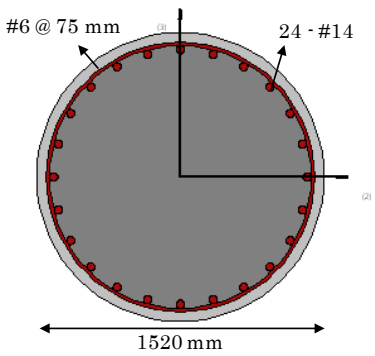

Figure 3: Figure shows the section used for all the columns in both bridges.

Bridge Model	Test ID
Bridge 1(Symmetric)	1-9, 19-22, 28-31, 37-38, 41-41
Bridge 2(Asymmetric)	10-18, 23-27, 32-36, 39-40

Table 2: Bridge models used in this study and the corresponding test numbers

The cap beams and girders were modeled using elastic frame elements with appropriate stiffness and mass characteristics. The girders were modeled as T-beams (6 in total) that were connected together laterally at equal intervals of 5 m using the *equaldof* constraint (in the transverse direction). The mass source for the models were assigned from the member self weights and were specified only in the transverse translation (y-direction) and vertical rotation (z-direction).No additional masses were defined. Damping was defined globally. Four different damping models used in this study were:

1. Initial stiffness proportional Rayleigh damping (ISR)
2. Tangent stiffness proportional Rayleigh damping (TSR)
3. Tangent stiffness proportional damping (TS)
4. No damping (NO)

Damping Model	Test ID
ISR	1, 3, 5, 7, 9, 11, 13, 15, 17, 37, 39, 41
TSR	2, 4, 6, 8, 10, 12, 14, 16, 18, 38, 40, 42
TS	19-27
NO	28-36

Table 3: Viscous damping models used in this study and the corresponding test numbers

Two different abutment fixity conditions were also included in the analysis. One was the free abutment condition where the abutment degrees-of-freedom were left unrestrained, while the other was the abutment restraint condition where all three abutment translational degrees-of-freedom were restrained.

Abutment Condition	Test ID
Free Abutment	1-4, 19-22, 28-31, 37-38, 41-42
Restrained Abutment	5-8, 15-18, 21-22, 26-27, 30-31, 35-40

Table 4: Bridge models used in this study and the corresponding test numbers

3.2 Ground motions used for analyses

Ground Motion	Test ID
Kocaeli x1	1-2, 9-10, 19, 23, 28, 32, 37-40
Kocaeli x2	3-6, 11-12, 15-16, 20-21, 24, 26, 29, 30, 33, 35
Kocaeli x3	7-8, 13-14, 17-18, 22, 25, 27, 31, 34, 36, 41-42

Table 5: Ground motions used in this study and the corresponding test numbers

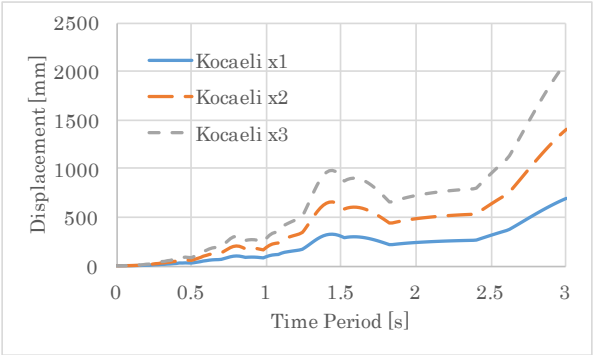

Figure 4: Figure shows the 5% damped displacement response spectrum for the different ground motions used in this study.

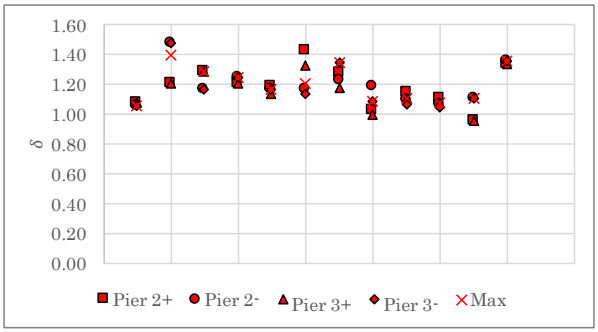

Figure 5: Displacement ratios (δ) for responses from NLTH analyses using TSR model.

An acceleration record from Kocaeli earthquake was chosen to be used in all the analyses. This was chosen as the record was available within the SEISMOSTRUCT libraries and the total time of the record was low, which would save time per analysis.To compare responses at different ductility levels, the same ground motion was scaled 1, 2 and 3 times to produce three different levels of earthquakes(Figure 4).

3.3 Displacement ratio

To be able to conduct a parametric study, a new parameter was defined. This is similar to the study in [3]. The displacement ratio (δ) is being defined as the ratio of any displacement response from an analysis conducted by using any viscous damping model to the corresponding response from the same analysis conducted using the initial stiffness proportional Rayleigh (ISR) damping model. For example, if we want to find the displacement ratio for a response obtained from an analysis using tangent stiffness proportional Rayleigh (TSR) damping model, we have,

$$\delta = \frac{\Delta_{TSR}}{\Delta_{ISR}} \tag{6}$$

This parameter, δ, allows us to easily check for the sensitivity of the results to different variable changes. All the results have been plot with respect to δ. A displacement ratio of greater than 1.0 means that the displacement responses from that particular analysis are higher than what one would observe when using the ISR model.

3.4 NLTH analysis and results

A total of 42 NLTH analyses were carried out for this study. The analysis matrix can be derived from Tables 2, 3, 4 and 5. The results obtained from each analysis were the maximum positive and negative displacements (maximum displacements to both sides) of the points of interest, which were the top points of Piers 2 and 3. The displacement ratio (δ) for each of these responses were obtained. Figure 5 plots δ for all the analyses obtained using the TSR model. It can be clearly seen that almost all data points are above 1.0. Some of the points even rise up to a value of 1.42. This is consistent with what has been observed for SDOF systems. Using TSR damping model predicts larger displacements as compared with those using ISR damping model.

Next, an attempt is made to check the behavior of δ with ground motion intensity as a variable. Figures 6a and 6b plot the results classified on the basis of ground motions used for analysis. While Figure 6a plots all the results, Figure 6b plots only the maximum responses. The accelerations go from lowest to highest from

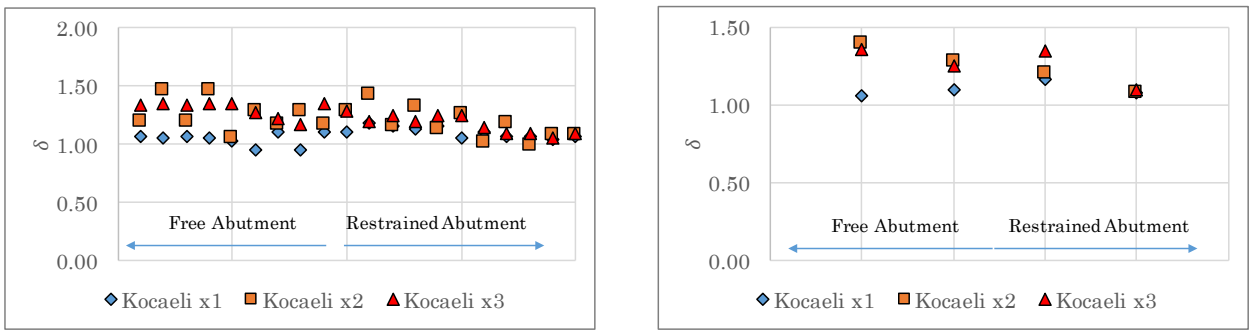

(a) (b)

Figure 6: δ characterized based on ground motion (a) All displacements and (b) Maximum displacements.

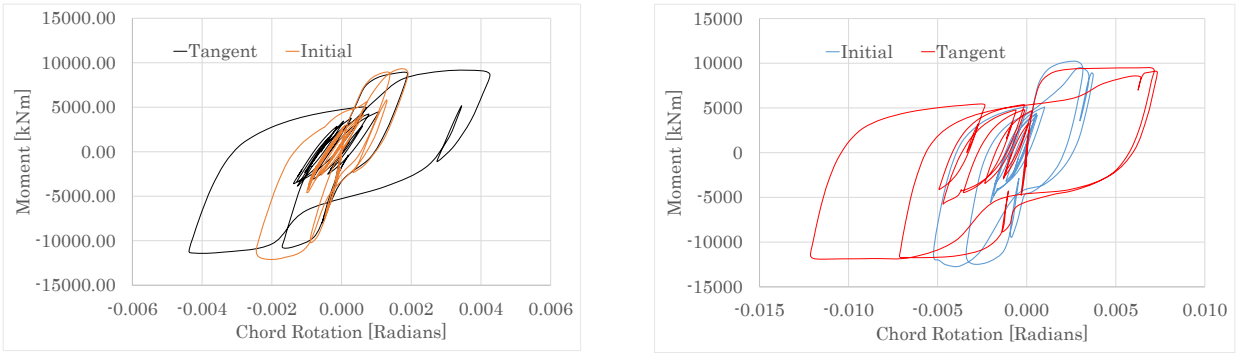

(a) (b)

Figure 7: Moment-rotation hysteresis in plastic hinge location (a) Kocaeli x2 and (b) Kocaeli x3.

Kocaeli x1 to Kocaeli x3. It was observed that Kocaeli x1 resulted in low ductility response (around the yield limit state), Kocaeli x2 in medium ductility (around the serviceability range) and Kocaeli x3 in high ductility (around the damage control limit state). It can be seen that Kocaeli x2 ground motion in a lot of cases cause a higher value of δ compared to Kocaeli x3. A couple of possible reasons for this may be as follows. Kocaeli x3 ground motion, causes high displacements resulting in higher ductility. It is thought that, at this level of ductility, the hysteretic damping component of the total damping may be significant enough to cause a lower variation between the responses obtained using the TSR model and the ISR model. Figure 7a and 7b illustrate this point. It can be clearly seen that the energy dissipation between "Tangent" and "Initial" loops for Kocaeli x3 ground motion is higher than that for Kocaeli x2. Nevertheless, this claim needs further investigation to be conclusive. A second reason may be the fact that the absolute magnitude of the displacements for Kocaeli x3 ground motion is much higher than that of Kocaeli x2. This means that even a small percentage deviation in Kocaeli x3 results can be of a higher significance. This also requires further investigation. A second observation that can be made regarding Figure 6 is that a higher scatter can be seen for the free abutment results compared to restrained abutments. More on this is discussed later.

Figure 8 classifies the same data based on the used bridge model. Bridge 1 is displayed as Symmetric and Bridge 2 as Asymmetric. In Figure 8a, clearly the values of δ for the symmetric bridge have a much higher scatter than those for asymmetric. In figure, 8b, except for those from Kocaeli x1 ground motion, δ for the symmetric model is higher. At this point, the reason for this is unknown. Although the pattern is striking, further investigation is required before any conclusions can be made. One explanation could be that it is just an artifact of comparing δ which is a ratio of absolute displacements without any normalization. Another observation is that restrained abutment condition shows lesser values of δ with less scatter compared to free abutment condition.

Figure 9 corroborates this observation. It can be said that in almost all cases, both Figure 9a and 9b, the displacement ratio (δ) is higher for free abutment bridges compared to restrained abutment bridges, given the other variables remain the same. Free abutment bridge results also show a higher scatter. A possible reason for this may be that restraining the abutments reduce the fundamental periods of the structure as well as lower the absolute maximum displacements. This contributes to a lower variation between results obtained by using the ISR model and the TSR model. Only for a combination of free abutment and asymmetric conditions can you observe the displacement ratio (δ) for Kocaeli x3 ground motion to be higher than that for Kocaeli x2.

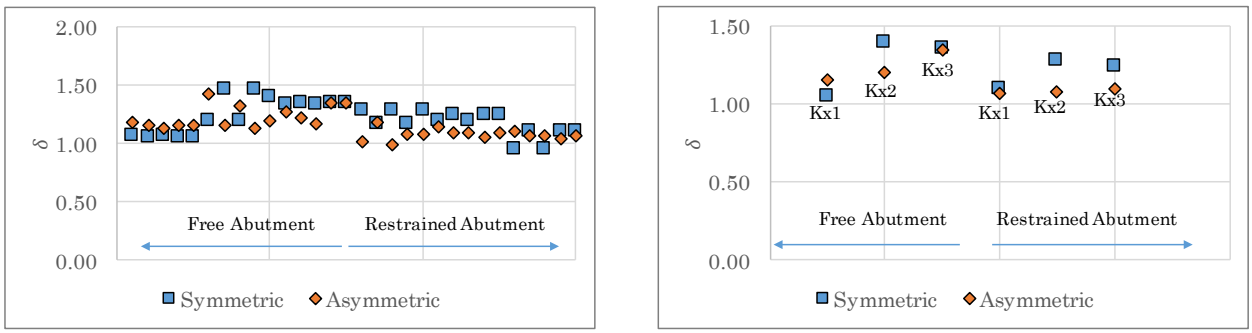

Figure 8: δ characterized based on bridge geometry - Symmetric and Asymmetric (a) All displacements and (b) Maximum displacements.

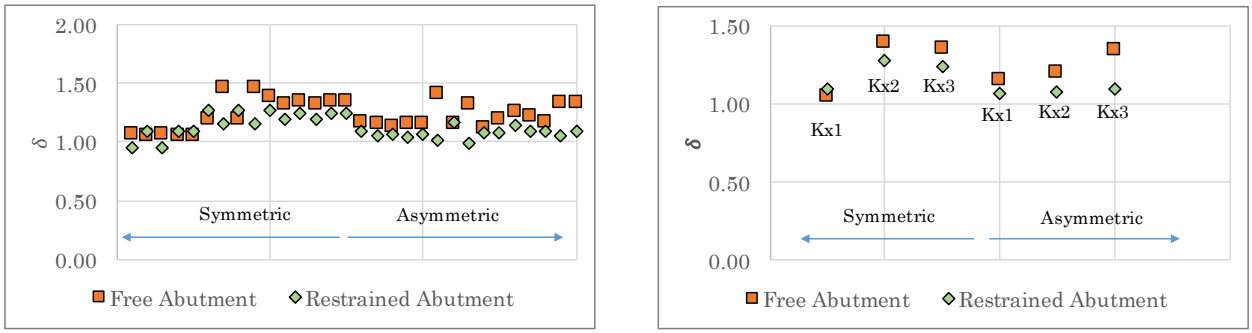

Figure 9: δ characterized based on abutment restraint condition - Free and Translational Restraint (a) All displacements and (b) Maximum displacements.

Two other damping models were also analyzed to get an idea about the behavior of the displacement ratio (δ). One was the TS model and the other was having no viscous damping, NO model. Only the overall results were plot similar to Figure 5 and were not investigated any further. Figures 10a and 10b show the results for TS and NO models respectively. It is worth noting that a good proportion of the points for displacement ratio (δ) lie below 1.0 when TS model is used. In all these cases, using TS model is under-predicting the displacements compared to the ISR model. This may be a by-product of how the program SEISMOSTRUCT employs this model. In the program, one has to manually enter a period and a corresponding damping ratio using which it calculates the stiffness parameter. This stiffness parameter is then used as the scaling factor for the stiffness matrix to obtain the damping matrix. Hence, if the period chosen is the first mode period and the response is dominated by the second mode, the resulting displacements will be lower as the effective damping ratio for the second mode would increase. Recall that the curve for stiffness proportional damping is a straight line with a positive slope.

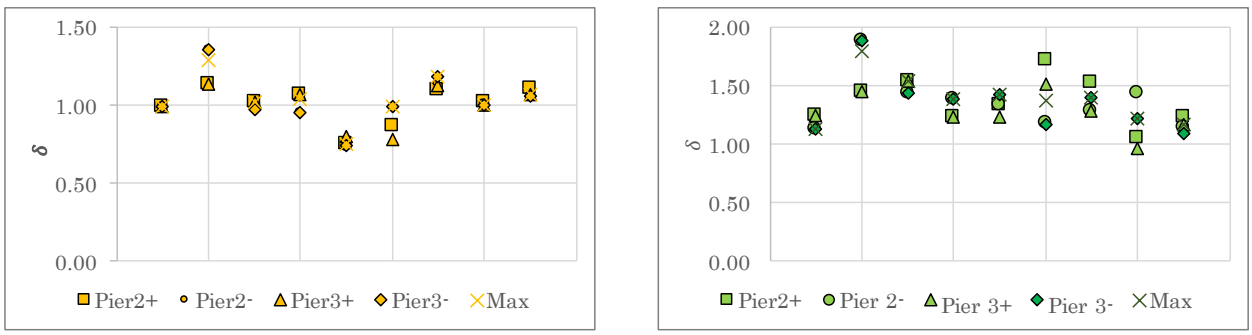

Figure 10: Displacement ratios (δ) for responses from NLTH analysis using (a) TS model and (b) NO model.

Petrini et al. [6] had also compared the shake table experimental results to predictions obtained by specifying no additional viscous damping model in their SDOF fiber based model (Figure 1b) giving better prediction than ISR model. This provided a motivation to employ the same in these MDOF fiber models. NO model would mean that no additional viscous damping is specified and the only damping in the analysis is contributed by hysteretic damping. An argument in support of using this in fiber based models is because of the fact that in the elastic range, one would still get some energy dissipation because of the material models. Like the TS model, NO (No damping) model was used to only get the overall plot (Figure 10b). It is observed that this would result in very high displacement ratio (δ) on many occasions. The question whether this is an over-prediction or closer to actual results can not be answered in this study.

4 Conclusions

This study aimed to obtain some preliminary results regarding the sensitivity of NLTH analysis response predictions of MDOF structures to the choice of viscous damping models. The sensitivity was characterized using a parameter called the displacement ratio (δ). The higher the value of δ, the higher the deviation of responses from the prediction obtained from ISR model. When the choice was the TSR model, for maximum displacements, a maximum of δ=1.39 and a minimum of δ=1.05 were obtained. For TS model, these values were 1.29 and 0.75 respectively. For NO model, these were 1.79 and 1.13 respectively. It can be inferred that, a choice of damping model does impact the response prediction. It can also be stated that, abutment fixity conditions and bridge geometry also play a part in determining the sensitivity. Three different ground motion intensities were used in the analyses and these also impacted the resulting δ values. Impact of all the variables above can be boiled down to an impact of a change in two important parameters: (a) The structural period and (b) member ductility. A future study could try to correlate the sensitivity to these two parameters. A point worth emphasizing is the importance of determining the structural periods and modal participation before any NLTH analysis if Rayleigh damping models are used in SEISMOSTRUCT. These have to be determined using both initial stiffness and a reduced secant stiffness. This data can then be used to fix the two frequencies required to define the Rayleigh model using the best judgment. It is understood that other programs are able to carry out more robust analyses for a study of this kind.

As a path forward, it is also suggested that a study can be undertaken with the aim of understanding the sensitivity to provide correction factors that may be used by engineers who are limited by few options in a commercial program. This study would require a wider dataset including more variables like long and irregular bridges, soil structure interaction and different ground motions. A validation of the 'correct' model to be used in NLTH analysis of MDOF structures could only be possible using data from actual shake table tests.

References

[1] Charney, F. A. Unintended consequences of modeling damping in structures. *Journal of structural engineering 134*, 4 (2008), 581–592.

[2] Hall, J. F. Problems encountered from the use (or misuse) of rayleigh damping. *Earthquake engineering & structural dynamics 35*, 5 (2006), 525–545.

[3] Hasgul, U., and Kowalsky, M. Impact of viscous damping models on nonlinear response of sdof systems.

[4] Mander, J. B., Priestley, M. J., and Park, R. Theoretical stress-strain model for confined concrete. *Journal of structural engineering 114*, 8 (1988), 1804–1826.

[5] Menegotto, M., and Pinto, P. Method of analysis for cyclically loaded rc plane frames including changes in geometry and non-elastic behavior of elements under combined normal force and bending. In *Proc. of IABSE symposium on resistance and ultimate deformability of structures acted on by well defined repeated loads* (1973), pp. 15–22.

[6] Petrini, L., Maggi, C., Priestley, M. N., and Calvi, G. M. Experimental verification of viscous damping modeling for inelastic time history analyzes. *Journal of Earthquake Engineering 12*, S1 (2008), 125–145.

[7] Priestley, M., and Grant, D. Viscous damping in seismic design and analysis. *Journal of Earthquake Engineering 9*, spec02 (2005), 229–255.

[8] SeismoSoft, S. A computer program for static and dynamic nonlinear analysis of framed structures. *Disponível online em: http://www. seismosoft. com* (2006).